AMS applications in nuclear astrophysics - new results for $^{13}C(n,\gamma)^{14}C$ and $^{14}N(n,p)^{14}C$

A. Wallner[1,2], K. Buczak[1], I. Dillmann[3], J. Feige[1], F. Käppeler[3], G. Korschinek[4], C. Lederer[1], A. Mengoni[5], U. Ott[6], M. Paul[7], G. Schätzel[1], P.Steier[1], H.P. Trautvetter[8]

[1] *VERA Laboratory, Faculty of Physics, University of Vienna, Austria*
[2] *Department of Nuclear Physics, Research School of Physics and Engineering, The Australian National University, Canberra, Australia*
[3] *Karlsruhe Institute of Technology (KIT), Campus Nord, Institut für Kernphysik, Karlsruhe, Germany*
[4] *Physik Department der Technischen Universität München, Germany*
[5] *International Atomic Energy Agency, Nuclear Data Section, Austria*
[6] *Max-Planck-Institute for Chemistry, Hahn-Meitner-Weg 1, D-55128 Mainz, Germany*
[7] *Racah Institute of Physics, Hebrew University, Jerusalem, Israel*
[8] *Ruhr University Bochum, Bochum, Gernany*

anton.wallner@univie.ac.at and anton.wallner@anu.edu.au

Abstract: The technique of accelerator mass spectrometry (AMS) offers a complementary tool for studying long-lived radionuclides in nuclear astrophysics: (1) as a tool for investigating nucleosynthesis in the laboratory; and (2) via a direct search of live long-lived radionuclides in terrestrial archives as signatures of recent nearby supernova-events. A key ingredient to our understanding of nucleosynthesis is accurate cross-section data. AMS was applied for measurements of the neutron-induced cross sections $^{13}C(n,\gamma)$ and $^{14}N(n,p)$, both leading to the long-lived radionuclide ^{14}C. Solid samples were irradiated at Karlsruhe Institute of Technology with neutrons closely resembling a Maxwell-Boltzmann distribution for kT=25 keV, and with neutrons of energies between 123 and 178 keV. After neutron activation the amount of ^{14}C nuclides in the samples was measured by AMS at the VERA (Vienna Environmental Research Accelerator) facility. Both reactions, $^{13}C(n,\gamma)^{14}C$ and $^{14}N(n,p)^{14}C$, act as neutron poisons in s-process nucleosynthesis. However, previous experimental data are discordant. The new data for both reactions tend to be slightly lower than previous measurements for the 25 keV Maxwell-Boltzmann energy distribution. For the higher neutron energies no data did exist for $^{13}C(n,\gamma)$. Model calculations indicate a strong resonance structure between 100 and 300 keV which was confirmed by our results. Very limited information is available for $^{14}N(n,p)$ at these energies. Our new data at 123 and 178 keV suggest lower cross sections than expected from previous experiments and data evaluations.

Keywords: neutron poison, $^{13}C(n,\gamma)^{14}C$, $^{14}N(n,p)^{14}C$, activation, AMS

1. Introduction

Nuclear data provide a key ingredient for nucleosynthesis calculations and for our understanding of the chemical evolution in our galaxy. Accelerator mass spectrometry (AMS) is a relatively new technique which can be applied for measuring cross sections of relevance to nucleosynthesis. For specific reactions the sensitivity of AMS offers a unique tool to pin down uncertainties, thus elucidating current open questions e.g. within the s- and p-process path. AMS has been introduced to laboratory experiments in nuclear astrophysics for studying production of ^{44}Ti from ^{40}Ca(α,γ) (Paul et al. 2003a, Nassar 2005, Nassar, Paul et al. 2006), of ^{26}Al via ^{25}Mg(p,γ) (Arazi et al. 2006) and for neutron capture reactions in the regime of s-process environments, e.g. ^{62}Ni(n,γ) (Nassar, Paul et al. 2005). More specifically, AMS has been applied recently for neutron-capture studies of ^{40}Ca, ^{62}Ni, ^{58}Ni, and ^{78}Se (Dillmann et al. 2009, 2010, Rugel 2007) and in a series of recently completed measurements (see e.g. Wallner et al. 2007, 2010).

AMS is also used in a different but closely related application, namely for the search of live supernova (SN)-produced radionuclides in terrestrial archives, which might be imprinted through a unique isotopic signature (Ellis et al. 1996, Korschinek et al. 1996). Depending on the half-life of the searched-for radionuclide, one can reach back in time a few million years when searching for live ^{60}Fe ($t_{1/2}$ = 2.62 Myr) (Rugel et al. 2009), or several hundred million years, if searching for longer-lived nuclides such as the pure r-process nuclide ^{244}Pu ($t_{1/2}$ = 81 Myr). Indeed measurements by Knie et al. found a clear signal of extraterrestrial ^{60}Fe in a deep-sea manganese crust (Knie et al. 2004). Other measurements e.g. for SN-produced ^{244}Pu did not provide clear evidence for such a signal yet (Paul et al. 2001, 03b, 07, C. Wallner et al. 2004), even with improved sensitivity in ^{244}Pu detection (A. Wallner et al., in preparation). However, new technical developments and new sample material now available triggered a series of new projects for the search of such radionuclides (Korschinek 2011, Feige et al. 2012, Bishop et al. 2011).

Here, we present new measurements for studying neutron capture on ^{13}C and the ^{14}N(n,p) reactions. Neutron capture cross sections on light elements are usually very low (of the order of some 10 to 100 μbarn in the keV neutron energy range). Both, ^{13}C and ^{14}N are primary nuclides which are produced by the star itself. Although the capture cross sections for ^{13}C and ^{14}N are small, their abundances are high, therefore such reactions need to be considered as potential neutron poisons for the s-process: ^{13}C(α,n) is the most important neutron source for the main s-process. While neutron capture on ^{12}C(n,γ)^{13}C will also take place simultaneously

with $^{13}C(n,\gamma)$, the produced ^{13}C will serve as a target for the $^{13}C(\alpha,n)^{16}O$ reaction and the neutron consumed in the preceding $^{12}C(n,\gamma)$ reaction will be recycled, and thus recovered (Iliadis 2007). This is not the case for $^{13}C(n,\gamma)$. Moreover, via this neutron capture reaction, two ingredients for s-process nucleosynthesis are removed: (1) the primary ^{13}C nuclide, which forms the target for the neutron production via $^{13}C(\alpha,n)$, is transformed to ^{14}C, and (2) a neutron is also consumed and missing for the s-process. For the second reaction studied in this work, $^{14}N(n,p)^{14}C$, we note that the cross section is about 100 times higher (ca. 2 mbarn for keV energies) than the typical neutron capture cross sections in this mass range (ca. 10 μbarn). Furthermore, $^{14}N(n,p)$ produces protons which subsequently destroy ^{13}C via $^{13}C(p,\gamma)$ and form a cycle with the reaction product being again ^{14}N. As such, this reaction represents the most important neutron poison in s-process nucleosynthesis.

We investigated both reactions in the energy range around 25 keV (simulating a Maxwell-Boltzmann distribution) and at two higher neutron energies around 125 and 170 keV (see Table 1). A combination of neutron activation at Karlsruhe Institute of Technology (KIT) and subsequent AMS measurement at the Univ. of Vienna was applied. This approach directly counts the produced ^{14}C atoms in the sample after the neutron activation rather than measuring the associated γ-radiation or the emitted protons during the irradiation.

2. Existing data for $^{13}C(n,\gamma)^{14}C$ and $^{14}N(n,p)^{14}C$

2.1 $^{13}C(n,\gamma)^{14}C$

An interesting feature of the $^{13}C(n,\gamma)^{14}C$ reaction is a strong resonance at E_n= 143 keV. If the width of the resonance is broad, interference effects between the resonance and direct capture contributions need to be taken into account. This is the case for $^{13}C(n,\gamma)^{14}C$ where the resonance at 143 keV interferes with the p-wave contribution of the direct capture. Previous experimental data and a comparison with calculation for $^{13}C(n,\gamma)^{14}C$ (Herndl et al. 1999) indicate that the total capture cross section is dominated by a p-wave resonant contribution at energies above 20 keV. The non-resonant contribution is considerably lower and agrees well with the value extrapolated by the 1/v law from the thermal cross section (Herndl et al. 1999). At temperatures above 0.3 GK the reaction rate is dominated by the 143 keV resonance, at lower temperatures p-wave and s-wave contributions are dominant. The calculations of (Herndl et al. 1999) show a satisfactory agreement with two previous experimental data (Shima et al. 1997, Raman et al. 1990) although the energy dependence of the cross section is somewhat different. A significant discrepancy is found if the calculations of Herndl et al. are compared to the most recent evaluation of JEFF-3.1 (=EAF2003) which suggests at the resonance a cross section value being about a factor of 25 higher than calculated by Herndl et al.

Only two experiments exist for $^{13}C(n,\gamma)$ for neutron energies in the keV range (Shima 1997, Raman 1990]. Both experiments are consistent, however, they indicate a decreasing energy dependence of the cross section between ~25 and ~60 keV, while the calculations favour an increase due to the influence from the direct p-wave and resonance contributions (see Figure 2).

2.2 $^{14}N(n,p)^{14}C$

Much more work exists for $^{14}N(n,p)^{14}C$ in the keV energy range (Koehler & O'Brien 1989, Brehm et al. 1988, Gibbons & Barschall 1959, Johnson & Macklin 1950, Kii et al. 1999, Sanami et al. 1997). Experimental data are available for energies up to 7 MeV and one additional data-point at 14.5 MeV. The measurements by (Koehler & O'Brien, 1989) support a 1/v energy dependence up to some 100 keV. Most other experimental data in the energy range between 10 and 200 keV show good agreement, however, one measurement by Brehm et al. (Brehm et al. 1988) indicates cross-section values approximately a factor of two to three lower in this energy range (see Figure 3). This has a great impact on ^{14}N as a neutron poison,

and also for its role on ^{19}F production, where the protons produced through $^{14}N(n,p)^{14}C$ play an important role in synthesizing ^{19}F. While a 10% uncertainty in the $^{14}N(n,p)$ cross section will not have a substantial impact in ^{19}F production (Lugaro 2004, 08), the uncertainties clearly become significant if one includes the data of Brehm et al.

3. Neutron activations at KIT

Neutrons of keV energy can be produced via the ^{7}Li(p,n)^{7}Be reaction neutrons by protons impinging on a thick Li target. As this reaction has its threshold at 1881 keV, selecting a proton energy close to this threshold value generates neutrons with energies just in the range of this energy difference. Under these conditions, the neutrons are emitted in a forward cone with energies spread according to kinematics and energy loss in the Li target. In a proper irradiation geometry a sample can be irradiated with neutrons whose integrated cross section is directly related to a Maxwellian-averaged cross section at an effective temperature of ~25-30 keV (Ratynski & Käppeler 1988). Such a setup was developed at KIT for direct cross section measurements and for activations with subsequent decay counting of the produced activities. In this way a comprehensive set of measurements relevant to s-process nucleosynthesis was performed at KIT (see also Käppeler et al. 2011).

Samples prepared from highly enriched ^{13}C graphite powder (>98% ^{13}C) were used for studying the ^{13}C(n,γ)^{14}C reaction. The graphite powder was enclosed in small Al containers 6 mm in diameter. Au foils served as monitors for the neutron fluence determination (Ratynski & Käppeler 1988) and were attached to the ^{13}C sample to form a stack of Au-^{13}C-Au. Similarly, for the ^{14}N(n,p) studies, uracil powder ($C_4H_4N_2O_2$) was pressed into pellets and a sandwich was formed again by Au-foils. Production of ^{14}C from ^{13}C(n,γ) was negligible when using uracil due to the low ^{13}C content and the much higher ^{14}N(n,p) cross sections compared to ^{13}C(n,γ).

Three different neutron energies were selected at KIT. First, a neutron energy distribution peaking at 25 keV was produced by protons with energy Ep= 1.912 MeV. Two higher neutron energies of ~125 and ~170 keV with a broad energy spread were produced from higher-energetic protons through the same ^{7}Li(p,n) reaction (see Table 1). A proton beam intensity of typically 100 μA and 5 to 7 days activation resulted in a fluence of ~10^{15} neutrons per cm^2. Table 1 lists the main parameters of the neutron activations for enriched ^{13}C and uracil samples.

sample	reaction	E_p	$<E_n>$	neutron fluence
^{13}C graphite-1	$^{13}C(n,\gamma)^{14}C$	1912 keV	25 keV-MB	1.38×10^{15} n cm^{-2}
^{13}C graphite-2	$^{13}C(n,\gamma)^{14}C$	1960 keV	128 keV	6.65×10^{14} n cm^{-2}
^{13}C graphite-3	$^{13}C(n,\gamma)^{14}C$	2000 keV	167 keV	4.67×10^{14} n cm^{-2}
Uracil-1	$^{14}N(n,p)^{14}C$	1912 keV	25 keV-MB	8.04×10^{14} n cm^{-2}
Uracil-2	$^{14}N(n,p)^{14}C$	1960 keV	123 keV	8.64×10^{14} n cm^{-2}
Uracil-3	$^{14}N(n,p)^{14}C$	2000 keV	178 keV	6.04×10^{14} n cm^{-2}

Tab. 1: Main parameters for the neutron irradiations at KIT. E_p denotes the proton energy in the ^{7}Li(p,n) reaction and $<E_n>$ the mean neutron energy. “25 keV-MB” means Maxwell-Boltzmann distribution for kT=25keV. “Fluence” gives the neutron fluence for the various samples using the ^{197}Au(n,γ) cross-section value for 25 keV-MB by Ratynski & Käppeler (1988), and for the higher energies the data from ENDF/B-VII were used. Note, a different mean neutron energy for the same proton energy may result due to a slightly different irradiation geometry.

4. Accelerator Mass Spectrometry Measurements

Accelerator Mass Spectrometry (AMS) is a mass spectrometric technique based on the use of a (tandem) accelerator. The advantage of AMS compared to other mass spectrometric techniques is that it does not suffer from molecular interferences due to the use of tandem accelerators and can even be used for separating specific atomic isobars. It offers a complementary tool to measure cross sections of nuclear reactions leading to radioactive nuclides, independent of their decay times or schemes. The AMS measurements have been performed at the Vienna Environmental Research Accelerator (VERA) which represents a state-of-the-art AMS facility based on a 3-MV tandem (Steier et al. 2005). VERA provides the ability for quantitative detection of nuclides over the whole mass range. Among the measured radioisotopes are ^{10}Be, ^{14}C, ^{26}Al, ^{36}Cl, ^{41}Ca, ^{55}Fe, ^{68}Ge, ^{129}I, ^{182}Hf, ^{202g}Pb, ^{210m}Bi, ^{229}Th, ^{231}Pa, ^{236}U and $^{239-244}$Pu, within a wide range of applications – e.g. from archaeology to climate research. In particular, since a few years nuclear astrophysics measurements are one of the main applications.

In combination with use of negative ions and the suppression of molecules by applying acceleration and charge exchange, AMS offers an excellent sensitivity. The measured quantity

in AMS is an isotope ratio, i.e. rare isotope versus stable isotope contents in a sample. Detection limits of 10^{-15} and below have been achieved for several nuclides which allow the detection of most cosmogenic isotopes at natural concentrations.

Decay counting becomes difficult in case of long-lived reaction products. However, as the technique of AMS does not measure decays but directly the number of produced radionuclides, it adds as an additional method for such measurements involving longer-lived radionuclides. Because this method is completely independent of other techniques AMS measurements provide important information on potential systematic uncertainties of previous measurements.

^{14}C AMS measurements are routinely performed in most AMS laboratories (e.g. for ^{14}C-dating). However, the samples from the neutron activations are different from above mentioned routine measurements: the ^{13}C graphite samples were about 10 000 times higher in the isotope ratio $^{13}C/^{12}C$ than natural samples (ca. 1% ^{13}C abundance in natural samples). Therefore, reference materials originating from the same ^{13}C graphite were produced from neutron activation at thermal energies. We studied in this way possible mass fractionation effects in the measurements which could lead to a systematic offset of the measured isotope ratio for such enriched materials. Also, the highly enriched ^{13}C sample produced a slightly higher AMS measurement background compared to data obtained from natural graphite (which is assumed to be ^{14}C free). We could demonstrate that the amount of ^{13}C produced in our neutron activated samples was high enough and background effects did not contribute to our final uncertainties (Wallner 2008, 2010). Moreover, while the ^{13}C graphite could directly be used for the AMS measurement, the uracil samples ($^{14}N(n,p)^{14}C$) required sample processing to produce graphite powder for the subsequent AMS measurement.

5. Results

Table 2 lists the measured $^{14}C/^{12}C$ isotope ratios for the various neutron activated samples. If we compare these values with typical measurement backgrounds in ^{14}C-AMS (a machine background of $^{14}C/^{12}C$ ~3×10^{-16} for unprocessed and ~10^{-15} for processed samples), it is evident that background will not introduce a significant uncertainty contribution. However, other effects, most importantly some potential outgassing of freshly produced ^{14}C if converted to ^{14}CO, could not be excluded a priory. We performed a series of tests which confirmed that there were negligible losses. More details on the AMS measurements will be published elsewhere.

reaction	<En>	$^{14}C/^{13}C$_AMS	σ_{exp} (µbarn)
	25 keV-MB	$(1.84 \pm 0.21)\times10^{-14}$	13.3 ± 1.5
$^{13}C(n,\gamma)^{14}C$	128 keV	$(9.1 \pm 0.6)\times10^{-14}$	137 ± 9
	167 keV	$(4.3 \pm 0.3)\times10^{-14}$	92 ± 7
reaction	**<En>**	**$^{14}C/^{12}C$_AMS**	**σ_{exp} (mbarn)**
	25 keV-MB	$(6.9 \pm 0.6)\times10^{-13}$	1.74 ± 0.15
$^{14}N(n,p)^{14}C$	123 keV	$(3.5 \pm 0.2)\times10^{-13}$	0.83 ± 0.07
	178 keV	$(2.6 \pm 0.2)\times10^{-13}$	0.88 ± 0.07

Tab. 2: Isotope ratios $^{14}C/^{12}C$ as measured via AMS. The cross section values are calculated according to equ. 1 and 2. No corrections for the finite neutron energy distributions have been applied yet. Note, uracil contains twice as much carbon than nitrogen (chemical formula: $C_4H_4N_2O_2$).

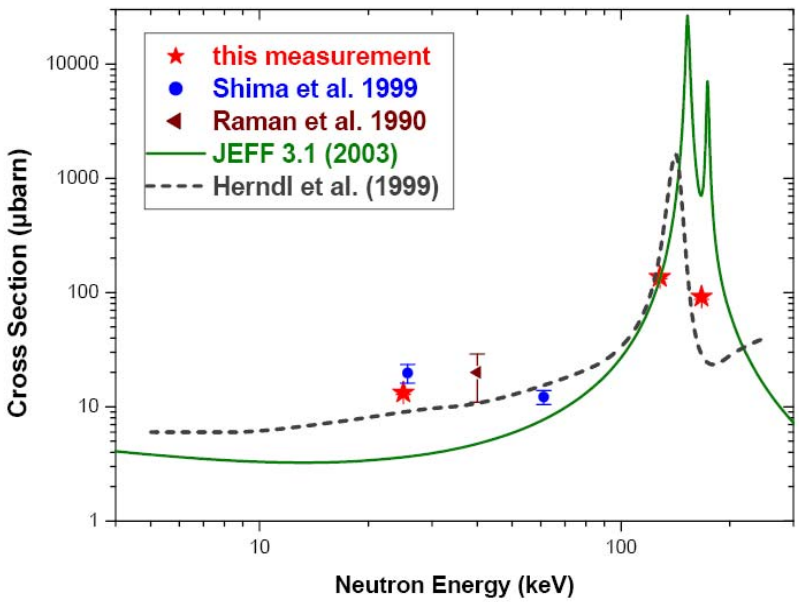

Fig. 1: Experimental data for $^{13}C(n,\gamma)^{14}C$ in the keV neutron energy region. Plotted are all published experimental data and the calculated values by (Herndl et al. 1999) and a recent evaluation (JEFF-3.1)

The experimental cross sections σ_{exp} can simply be calculated from the following equations

$$\sigma_{exp} = \frac{^{14}C}{^{13}C} \times \frac{1}{\Phi} \qquad (1)$$

and

$$\sigma_{exp} = \frac{^{14}C}{^{14}N} \times \frac{1}{\Phi} \qquad (2),$$

where $^{14}C/^{13}C$ and $^{14}C/^{14}N$ denote the isotope ratios measured via AMS, respectively, and Φ the neutron fluence; the latter was determined from Au monitor foils via $^{197}Au(n,\gamma)$ (Ratynski & Käppeler 1988). Note, the actual measured isotope ratio for $^{14}N(n,p)^{14}C$ is the ratio $^{14}C/^{12}C$, which is directly correlated to the number of ^{14}N atoms, as for uracil ($C_4H_4N_2O_2$) $^{12}C/^{14}N$ = 1.98 (99% ^{12}C, 1% ^{13}C) and therefore, the AMS results are all mass independent. Data listed in Table 2 are preliminary data, as they are calculated from the product of neutron fluence and isotope ratio only. The broad neutron energy distributions, specific for the various

activations, still need to be modelled. This work is now in progress. The final AMS data are expected to be precise to better than 2% for both reactions.

In Figure 1 our data (stars) for $^{13}C(n,\gamma)^{14}C$ are plotted in comparison with calculations (Herndl et al. 1999, dashed line), an evaluation (JEFF-3.1, solid line) and previous experimental results (Shima et al. 1999, Raman et al. 1990). Taking into account, that our data are still not adjusted for the finite neutron energy distribution, they indicate good agreement with previous data while the JEFF data are about a factor of three lower for 25 keV. Similarly, the two results at the higher neutron energies near the resonance fit well to the calculation by (Herndl et al. 1999). The final uncertainties of our data will be dominated by the uncertainty resulting from folding the neutron energy distribution with the experimental value.

The new data for $^{14}N(n,p)$ (stars) are plotted in Figure 2 together with previous experimental data and semi-empirical evaluations. At 25 keV we find a value slightly lower but close to recent experimental data. Our data do not confirm the data published by Brehm et al. (1988). At the higher neutron energies at 123 and 178 keV, respectively, our data suggest a factor of two lower values as the two previous experiments (Johnson & Barschall 1950, Gibbons & Macklin 1959) indicate.

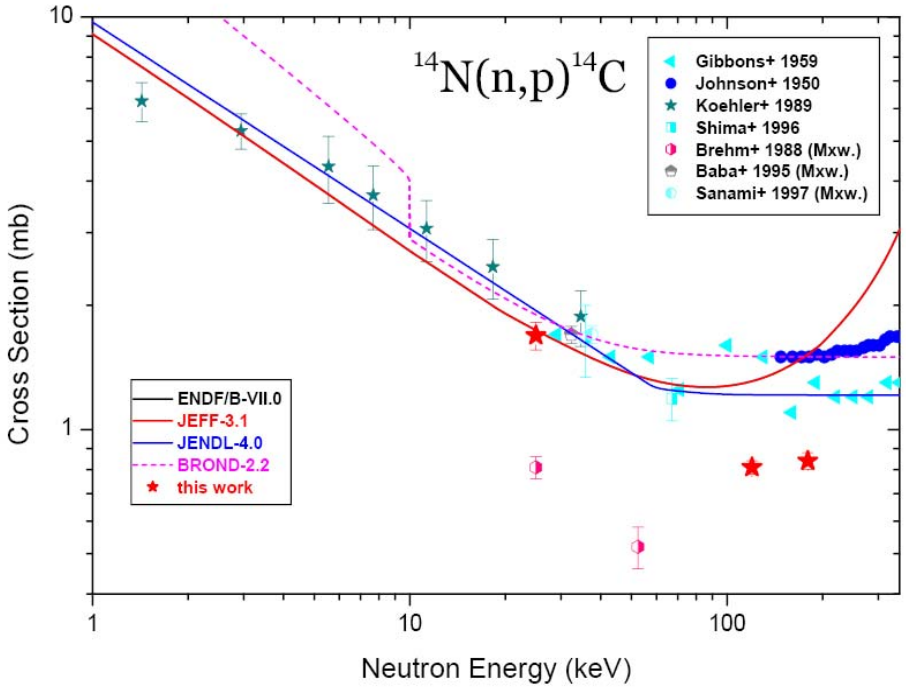

Fig. 2: Experimental data and recent evaluations for $^{14}N(n,p)$ in the neutron energy range between 1 and 350 keV.

6. AMS and nuclear astrophysics – summary and outlook

Recent AMS measurements have provided data for open questions in nuclear astrophysics (e.g. Nassar et al. 2005, Dillmann et al 2010; for a summary of recent AMS measurements see Wallner 2010). In the present work we exemplified this technique via measurements of the $^{13}C(n,\gamma)$ and $^{14}N(n,p)$ reactions. Samples containing ^{13}C and ^{14}N were irradiated at Karlsruhe Institute of Technology with neutrons neutrons having an energy distribution allowing the direct determination of a Maxwellian-averaged cross section, and also with broad neutron energy distributions between 123 and 178 keV mean energy. After the neutron activation the amount of ^{14}C produced was quantitatively determined by AMS. $^{13}C(n,\gamma)^{14}C$ and $^{14}N(n,p)^{14}C$ reactions act both as neutron poisons in s-process nucleosynthesis, while $^{14}N(n,p)$ also serves as a proton donator, leading to a delayed neutron recycling, and the protons released are important for the production of ^{19}F as well. New data were obtained for $^{13}C(n,\gamma)$ at 25 keV, and also first experimental results for 128 and 167 keV neutron energy, where a strong resonance is predicted. The reaction $^{14}N(n,p)^{14}C$ was measured at similar neutron energies, 25 keV Maxwell-Boltzmann and at 123 and 178 keV. The new results obtained with AMS are slightly lower at 25 keV and significantly lower at the higher neutron energies than most previous experimental results. Additional AMS measurements were performed recently at VERA for the neutron capture reactions $^{9}Be(n,\gamma)$, $^{35}Cl(n,\gamma)$, $^{54}Fe(n,\gamma)$ and $^{209}Bi(n,\gamma)$.

In another approach AMS provides a sensitive technique to search for live radionuclides in terrestrial archives (Knie et al. 2004, Paul et al. 2007). AMS will also play an important role within the European Eurogenesis Research Programme 'Cosmic Dust as a Diagnostic for Massive Stars' (CoDustMas). This project comprises the laboratory study of cosmic dust via AMS measurements at University of Vienna, TU Munich, ETH Zurich, MPI Mainz, Hebrew University, and the Australian National University (Canberra). Two aspects are investigated within this project: (1) the measurement of trace element isotope ratios in presolar nanodiamonds isolated from meteorites (stardust), e.g. isotope ratios of Pt isotopes to extract r-process nucleosynthesis signatures (Ott et al. 2012, Wallner et al. 2011); and (2) the search for live supernova (SN)-produced radionuclides in terrestrial deep-sea archives (Feige et al. 2012).

Acknowledgement

This work was partly funded by the Austrian Science Fund (FWF), project No. P20434 and I428.

References

Arazi, A. et al. 2006, Phys. Rev. C74, 025802

Bishop J. & Egli R. 2012, The Astrophys. Journal Letters, 738, L32

Brehm K. et al. 1988, Z. Phys. A 330, 167

Dillmann, I. et al. 2009, Phys. Rev.C79, 065805

Dillmann, I. et al. 2010, Nucl. Instr. Meth. B268, 1283

Ellis, J., Fields B.D., & Schramm, D.N. 1996, Astrophys. J. 470, 1227

ENDF, Evaluated Nuclear Data File", http://www-nds.iaea.org/exfor/endf00.htm

Feige J. et al. 2012, these proceedings

Gibbons, J.H. & Macklin, R.L. 1959, Phys. Rev. 114, 571

Herndl, H., R. Hofinger, J. Jan, H. Oberhummer, J. Görres, M. Wiescher, F.K. Thielemann, B.A. Brown 1999, Phys. Rev. C60, 064614

Iliadis, C. 2007, Nuclear Physics of Stars, Wiley-VCH Verlag GmbH & Co. KGaA, Weinheim, ISBN: 978-3-527-40602-9, p. 518 ff.

Johnson, C.H. & Barschall, H.H. 1950, Phys. Rev. 80, 818

Käppeler, F., Gallino, R., Bisterzo, S. & Aoki, W. 2011, Rev. Mod. Phys. 83, 157.

Kii, T., Shima, T., Sato, H., Baba, T. & Nagai, Y. 1999, Phys. Rev. C59, 3397.

Knie, K. et al. 2004, Phys. Rev. Lett. 93, 171103.

Koehler P.E. & O'Brien, H.A. 1989, Phys. Rev. C39, 1655

Korschinek, G. et al. 1996, Radiocarbon 38, 68

Korschinek, G. 2011, unpublished

Lugaro, M. et al 2004, The Astrophys. J 615, 934.

Lugaro, M. et al. 2008, Astron & Astrophys 484 (2008) L27

Nassar, H. et al. 2004, Nucl. Phys. A746, 613c

Nassar, H. et al. 2005, Nucl. Phys. A758, 411

Nassar, H., M. Paul et al. 2005, Phys. Rev. Lett. 94, 092504

Nassar, H., M. Paul et al. 2006, Phys. Rev. Lett. 96, 041102

Ott, U. et al. 2012, these proceedings

Paul, M. et al. 2001, Astrophys. J. Lett. 558, L133

Paul, M. et al. 2003a, Nucl. Phys. A718, 239c

Paul, M. et al. 2003b, Nucl. Phys. A719, C29

Paul, M. et al. 2007, J. of Radioanal. and Nucl. Chem. 272, 243

Raman, S., M. Igashira, Y. Dozono, H. Kitazawa, & J.E. Lynn 1990, Phys. Rev. C 41, 458

Ratynski, W. & Käppeler, F. 1988 Phys. Rev. C37, 595

Rugel, G. et al. 2007, Nucl. Instr. and Meth. B259, 683

Rugel, G. et al. 2009, Phys. Rev. Lett. 103, 7.

Sanami T. et al. 1997, Nucl. Instr. Meth. A394, 368

Shima, T., Watanabe K., Irie T., Sato H. & Nagai Y. 1995, Nucl. Instr. Meth. A356, 347

Shima, T., F. Okazaki, T. Kikuchi, T. Kobayashi, T. Kii, T. Baba, Y. Nagai, and M. Igashira 1997, Nucl. Phys. A621, 231c

Steier, P. et al. 2005, Nucl. Instr. and Meth. B240, 445.

Wallner, A. et al. 2007, Nucl. Instr. and Meth. B259, 677

Wallner, A. et al. 2008, Journal of Physics G 35, 014018.

Wallner, A. 2010, Nucl. Instr. and Meth. B 268, 1277.

Wallner, A. et al. 2011, Nucl. Instr. and Meth. B, submitted

Wallner, C., T. Faestermann, U. Gerstmann, K. Knie, G. Korschinek, C. Lierse, G. Rugel 2004, New Astr. Rev. 48, 145.